

UDC 539.3

V.A. Bazhenov¹, Doctor of Sciences**N.A. Solovei**¹, Doctor of Sciences**O.P. Krivenko**¹, Ph.D

¹*Kyiv National University of Construction and Architecture
31 Povitroflotsky Avenue, Kyiv, Ukraine, 03680*

MODELING OF NONLINEAR DEFORMATION AND BUCKLING OF ELASTIC INHOMOGENEOUS SHELLS

The paper outlines the fundamentals of the method of solving static problems of geometrically nonlinear deformation, buckling, and postbuckling behavior of thin thermoelastic inhomogeneous shells with complex-shaped mid-surface, geometrical features throughout the thickness, and multilayer structure under complex thermomechanical loading. The method is based on the geometrically nonlinear equations of three-dimensional thermoelasticity and the moment finite-element scheme. The method is justified numerically. Comparing solutions with those obtained by other authors and by software LIRA and SCAD is conducted.

Key words: geometrically nonlinear deformation, buckling, thin elastic inhomogeneous shell, thermomechanical load.

Introduction

The trends in the development of structural engineering and the design of thin-walled shell structures call for refined numerical methods for the analysis of the nonlinear deformation and buckling of various shells. Real shell structures are made inhomogeneous (smoothly-variable and stepwise-varying thickness, knees, ribs, cover plates, holes, cavities, channels, facets, layers) to enhance reliability and reduce materials consumption. Thermal fields may cause substantial strains and affect the mode of and time to buckling.

The present paper outlines a method for and results of solving static problems of nonlinear deformation and buckling of various shells subject to mechanical and thermal loads, because of uniform methodological positions of the 3-d geometrically nonlinear theory of thermoelasticity and the finite-element method (FEM) [4-12, 32, 50-55, 60-64].

The stability of shells is addressed in many studies [1, 14, 17, 19, 22, 24, 25, 31], where various assumptions are made to simplify problem solving. A few studies are concerned with the thermal stability of shells of simple geometry [2, 15, 16, 19, 22, 42, 46]. The three-dimensional approach to the study of shells is addressed in the monographs [20, 28, 37, 47], papers [29, 34, 36], and reports [33, 38, 39], which have recently increased in number. The three-dimensional nonlinear deformation and buckling of inhomogeneous shells were studied in a few publications [9, 36, 37]. In the

FEM, this approach involves creation of design models based on universal spatial finite elements (FEs) [13, 29, 36, 37, 39, 52, 60-64].

1. Problem Formulation

1.1. Basic Principles and Hypothesis. We will solve static problems of the stress–strain state (SSS), buckling, and postbuckling behavior of a wide class of thin inhomogeneous shells subject to external mechanical loads and nonuniform bulk heating. The SSS of a shell and its structural elements at all stages of loading in both prebuckling and postbuckling domains is determined using the geometrically nonlinear equations of the three-dimensional theory of thermoelasticity and taking into account all nonlinear terms and all the components of the strain and stress tensors. By the inhomogeneity of a shell is meant that (i) its thickness is continuously or stepwise variable and (ii) it consists of combinations of multilayer stacks along the thickness and in plan. The casing of the shell and the ribs reinforcing it can consist of an arbitrary number of layers of varying thickness bonded into a single piece. Each layer can be anisotropic and different from the others. Thus, thin multilayer shells of variable thickness and complex geometry are considered as three-dimensional bodies that can be reinforced with ribs and cover plates, weakened by cavities, channels, and holes, and have sharp bends in the mid-surface (Fig. 1).

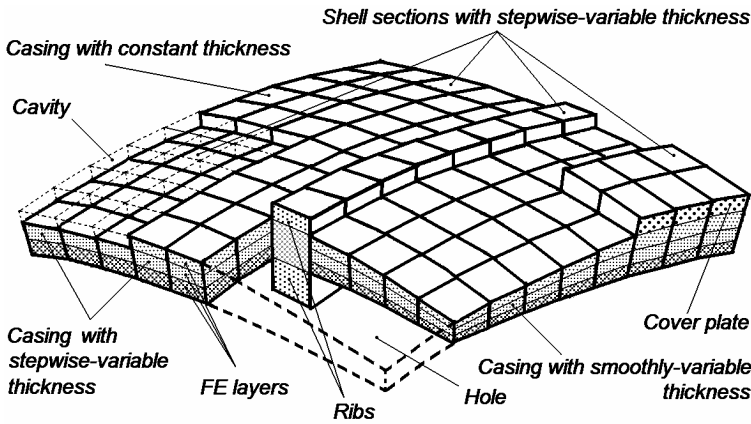


Fig. 1

The SSS of the shell is represented in a local curvilinear coordinate system x^i with basis $\bar{e}_i = \partial \bar{r} / \partial x^i$ and a global Cartesian coordinate system $x^{i'}$ with basis $\bar{e}_{k'} = \partial \bar{r} / \partial x^{k'}$ (Fig. 2) [61, 64].

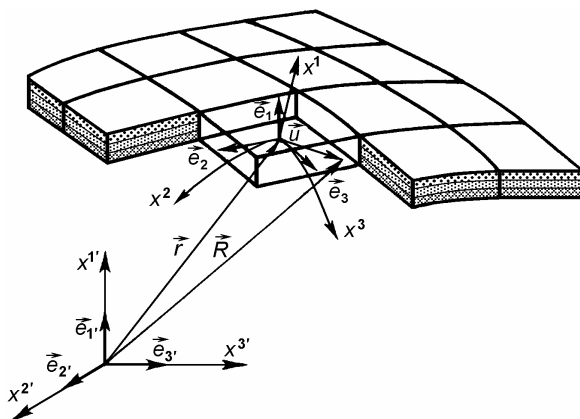


Fig. 2

The nonlinear deformation of shells is analyzed using the incremental method based on the general Lagrangian formulation where the trajectories of the strain and stress vectors are constructed using the increments of finite strains and stresses in the basis of the Lagrangian (reference) coordinate system [61, 64].

Two hypotheses are used to describe the SSS of a thin inhomogeneous shell.

The nonclassical kinematic hypothesis of deformed straight line: though stretched or shortened during deformation, a straight segment along the thickness remains straight. This segment is not necessarily normal to the mid-surface of the shell. The displacements are assumed distributed linearly along the thickness, which is conventional in the theory of thin shells [41]. The layers are bonded into a single piece so that there is no slippage and separation between them and the components of the displacement vector are equal at the interfaces. With certain restrictions on the material properties of the layers, this assumption leads to quite accurate solutions of the problems of buckling and vibration of thin multilayer shells [13, 45]. The hypothesis allows us to join spatial FEs keeping compatibility of the coordinates and displacements and to naturally model sharp bends, inclined walls of ribs, cavities, and holes.

The static hypothesis compressive assumes that the stresses σ_n^{11} in the fibers of the n th layer are constant throughout the thickness (along the x^1 -axis):

$$\frac{\partial \sigma_n^{11}}{\partial x^1} = 0. \quad (1.1)$$

Consider a steady-state thermal process, in which the temperature field in the shell is a known function of coordinates, $T=T(x^i)$, independent of the SSS [61,64]. Since the shell is thin, the temperature may be considered linearly distributed throughout the thickness of the layer. The effect of the mechanical and thermal fields on the shell is represented as a single process of loading described by a relationship between the general load parameter and the parameters of mechanical and temperature fields. The shell is modeled by a nonlinear elastic continuum subject to large displacements and small strains whose components are linear functions of stresses. The layers of the shell are considered linear elastic and described by the generalized Duhamel–Neumann law [40]

$$\sigma^{ij} = C^{ijkl} \varepsilon_{kl}^e = C^{ijkl} (\varepsilon_{kl} - \varepsilon_{kl}^T) = C^{ijkl} (\varepsilon_{kl} - \alpha_{kl} T) = \bar{\sigma}^{ij} - \overset{T}{\sigma}^{ij}; \quad (1.2)$$

$$\varepsilon_{ij} = \frac{1}{2} (C_j^{k'} \partial u^{k'} / \partial x^i + C_i^{k'} \partial u^{k'} / \partial x^j) + \frac{1}{2} (\partial u^{k'} / \partial x^i) \cdot (\partial u^{k'} / \partial x^j), \quad (1.3)$$

where ε_{kl}^e is the tensor of elastic strains related to internal stresses σ^{ij} ; ε_{kl} is the tensor of finite (total) Cauchy–Green strains; ε_{kl}^T is the tensor of thermal strains induced by a change in the initial temperature T_0 by T ; $\bar{\sigma}^{ij} = C^{ijkl} \varepsilon_{kl}$ are stresses dependent on total strains; $\overset{T}{\sigma}^{ij} = C^{ijkl} \alpha_{kl} T$ are stresses dependent on thermal strains; C^{ijkl} are the components of the stiffness tensor; α_{kl} are the components of the tensor of thermal-expansion coefficients; $C_i^{k'} = \partial x^{k'} / \partial x^i$ are the components of the coordinate transformation tensor; and $u^{k'}$ are the displacements in the Cartesian coordinate system.

The anisotropic inhomogeneous material of the shell is modeled by isotropic, transversely isotropic, and orthotropic materials of its layers [51,64].

1.2. The Universal Spatial FE and its Parameters. To develop a finite-element shell model (FESM), we approximate a thin shell by one spatial FE throughout the thickness, which is an efficient approach [13,20,28,36,37,39,48, 52,61,64]. The structural elements of an inhomogeneous shell require that the FE be universal: it should be eccentrically arranged relative to the mid-surfaces of the casing, it should be possible to vary the thickness of the lateral edges of the FE; the lateral edges of the neighboring FEs should be in continuous contact; and it should be possible to model sharp bends in and the multilayer structure of the shell.

The universal FE (Fig. 3) is based on an isoparametric spatial FE with polylinear shape functions for coordinates and displacements [52, 61, 64]. Additional variable parameters are introduced to enhance the capabilities of the modified FE. According to its constant and variable topological, geometrical,

and mechanical parameters, the FE is three-dimensional and has 8 nodes, 6 faces, and 12 edges with set material constants of homogeneous layers, mesh (s_k), local (x^k), and Cartesian ($x^{i'}$) coordinates of nodes (Fig. 3,*a,b*).

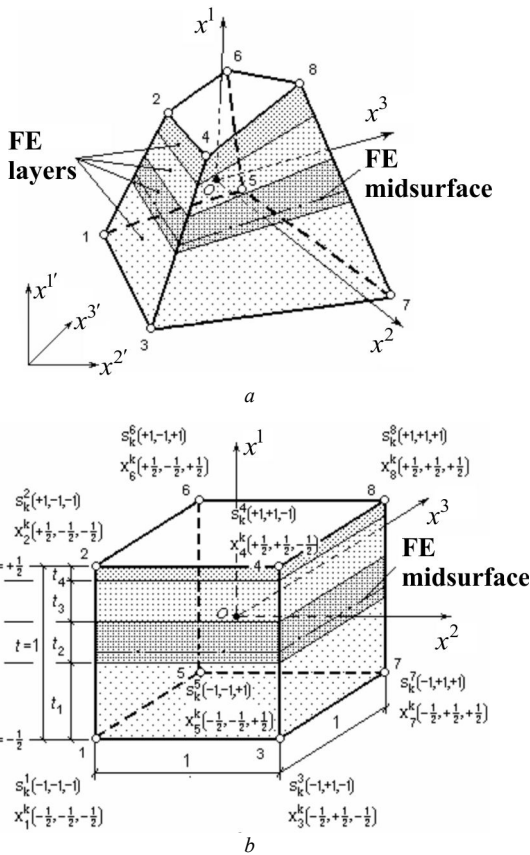


Fig. 3

The geometry of the FESM is set in two stages: (i) the Cartesian coordinates of the nodes on the bounding surfaces of the FE of the casing (SFE is a hexahedron $ABCDEFGH$, Fig. 4) are set; (ii) on sections with stepwise-variable thickness, the nodal coordinates of the SFE along the x^1 -axis are replaced by the nodal coordinates of the modified FE (MFE is a hexahedron

$\tilde{A}\tilde{B}\tilde{C}\tilde{D}\tilde{E}\tilde{F}\tilde{G}\tilde{H}$). The SFE is transformed into MFE by replacing the edges of the SFE (AB, CD, EF, GH) by the edges of the MFE ($\tilde{A}\tilde{B}, \tilde{C}\tilde{D}, \tilde{E}\tilde{F}, \tilde{G}\tilde{H}$).

By varying the additional parameters, the modified spatial FE is endowed with the properties of a universal FE, which allows unified modeling of a wide class of inhomogeneous shell structures. The idea of transforming a SFE into a MFE may be used as an example for the creation of other universal FEs.

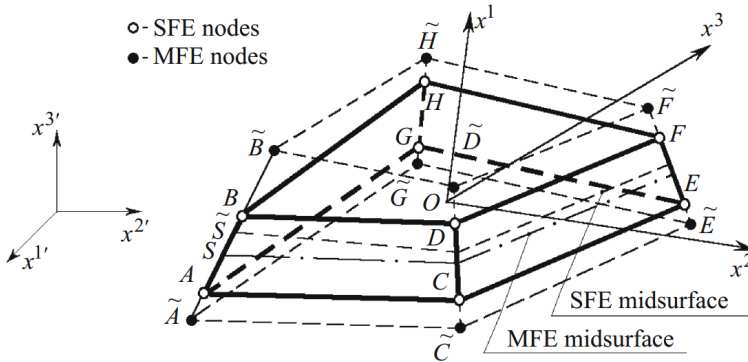


Fig. 4

1.3. The Moment Finite-Element Scheme at the Problems of Thermoelastic Deformation of Inhomogeneous Shells. To derive the governing finite-element equations for displacements, use is made of the moment finite-element scheme (MFES) developed and theoretically proved by Sakharov [37, 49]. The MFES is applied to thin multilayer shells of stepwise-variable thickness undergoing geometrically nonlinear deformation under thermomechanical loads [8, 9, 11, 32, 55, 61, 64]. The MFES approximations of displacements and strains guarantee a correct description of the rigid-body displacements of FEs, which enhances the convergence and accuracy of solutions on coarse meshes.

The MFES represents the total strains (1.3) as truncated Maclaurin series about the FE center. So strains are defined within a FE as linear functions of x^i . Those terms that can be exactly calculated in the case of polylinear displacements are retained in the series.

The thermal strains ε_{ij}^T , which depend on both temperature and material properties of the layer, are assumed to be linear functions of the coordinates x^2 and x^3 within a FE and in stepwise-linear functions of the coordinate x^1 [9, 11, 61, 64]. They are expanded into a Taylor series about the center of the n th layer.

Stresses are represented as linear parts of a Taylor series in powers of local coordinates x^i about the center of the n th layer.

2. FEM Equations for Elastic Inhomogeneous Shells Undergoing Geometrically Nonlinear Deformation

2.1. FEM Equations for Thin Inhomogeneous Shells. The nonlinear deformation of a shell is considered as a sequence of equilibrium states during steps of loading. The history of the SSS and the geometry of the shell are assumed known at the current step of loading. The equilibrium state of the FESM is determined based on the virtual-displacement principle and the Lagrange equation

$$\delta \Pi = \sum_{FE} (\delta W_{FE} - \delta A_{FE}) = 0, \quad (2.1)$$

here Π is the strain energy of the FESM; W_{FE} and A_{FE} are the works done by internal and external forces of a FE; \sum_{FE} is the sum over finite elements of the FESM.

With (1.2), the virtual work of internal forces is given by

$$\begin{aligned} \delta W_{FE} &= \int_{V_{FE}} \sigma^{ij} \delta(\varepsilon_{ij} - \varepsilon_{ij}^T) dv = \int_{V_{FE}} \sigma^{ij} \delta \varepsilon_{ij} dv = \\ &= \int_{V_{FE}} \bar{\sigma}^{ij} \delta \varepsilon_{ij} dv - \int_{V_{FE}} \bar{\sigma}^{ij} \delta \varepsilon_{ij}^T dv = \delta \bar{W}_{FE} - \delta \bar{W}_{FE}^T. \end{aligned} \quad (2.2)$$

With (2.2), Eq. (2.1) is represented as

$$\delta \Pi = \sum_{FE} (\delta \bar{W}_{FE} - \delta P_{FE}) = 0; \quad \delta P_{FE} = \delta A_{FE} + \delta \bar{W}_{FE}^T. \quad (2.3)$$

Equation (2.3) is integrated in a manner standard for the FEM. The reaction matrix of a FE is derived from the expression for the virtual work done by the internal forces due to the total strains dependent on the nodal displacements. The virtual work of internal forces due to thermal strains is used to determine the matrix of equivalent thermal loads, which supplements the matrix of mechanical nodal loads.

It is common practice to use the Cartesian displacements $u_{s_1 s_2 s_3}^{t'}$ of FE nodes as unknowns for a spatial FE. For thin shells, it is expedient to use, as unknown functions, the set of displacements of nodal points on the mid-surface $v_{s_2 s_3}^{t'}$ and the differences of nodal displacements $v_{s_2 s_3}^{t'}$ on the bounding surfaces of a FE:

$$v_{s_2 s_3}^{t'} = \frac{u_{s_1=+1s_2s_3}^{t'} + u_{s_1=-1s_2s_3}^{t'}}{2}; \quad v_{s_2 s_3}^{t'} = u_{s_1=+1s_2s_3}^{t'} - u_{s_1=-1s_2s_3}^{t'}. \quad (2.4)$$

Replacement (2.4) is considered as a changeover from an eight-node spatial FE with three nodal displacements to a four-node shell FE with six generalized displacements of nodes referred to the mid-surface of the FE. The triple linear approximation of displacements, strains, and stresses allows us to integrate (2.2) analytically and to obtain the explicit matrices of reactions, stiffness, geometrical stiffness, and equivalent thermal loads, which made it easier to calculate them. The equations derived for the spatial FE are universal because they are independent of the nodal coordinates and displacements, the number of layers, and engineering constants of layers. The characteristics of the FE and associated additional parameters somehow appear in these equations. This makes it possible to apply the FEM equations to all structural elements of an inhomogeneous shell in deriving the governing system of geometrically nonlinear equations.

Iterative algorithms for solving systems of nonlinear FEM equations are based on multiple solution of linearized systems of equations [23, 37, 54]. By linearizing the nonlinear FEM equations, we obtain, in analytic form, the stiffness matrix and the matrix of geometrical stiffness for the spatial FE. Adding the matrix of geometrical stiffness allows more accurate initial approximations in the iterative procedure and almost halves the number of iterations at a step of loading. It is also possible to increase the step.

2.2. Correcting the FEM Equations for the Modified FE. Deriving the system of governing nonlinear equations for the FESM involves uniting various combinations of SFE and MFE into a single ensemble of elements and matching of the nodal generalized displacements referred to the mid-surfaces of the SFE and MFE using the relationship between the generalized displacements of the SFE and MFE and the respective coefficients of the matrices of the SFE and MFE.

The generalized nodal displacements $v_{s_2s_3}^{i'}$ and $v_{s_2s_3}^{i'}$ of the mid-surface (datum surface) of the FESM casing are used as the variables of the system of governing nonlinear equations. The generalized displacements of the MFE are denoted by $\tilde{v}_{s_2s_3}^{i'}$ and $\tilde{v}_{s_2s_3}^{i'}$. The generalized nodal displacements of the SFE and MFE are related by

$$\tilde{v}_{s_2s_3}^{i'} = v_{s_2s_3}^{i'} + a_{s_2s_3} v_{s_2s_3}^{i'} ; \quad \tilde{v}_{s_2s_3}^{i'} = b_{s_2s_3} v_{s_2s_3}^{i'} , \quad (2.5)$$

where $b_{s_2s_3}$ is a coefficient of change in the length of the FE edge, and $a_{s_2s_3}$ is the ratio of the displacement of the FE edge to its length. These quantities are the additional parameters of the universal FE.

Relation (2.5) are the compatibility and continuity conditions for the displacements between all finite elements of the FESM on different sections of a shell with smoothly varying and stepwise-varying thickness.

3. Algorithm for Solving Problems of Nonlinear Deformation, Buckling, and Postbuckling Behavior of Shells under Thermomechanical Loading

3.1. Combined Algorithm for Solving a Nonlinear Buckling Problem. A few studies [37, 44, 54, 58, 61, 64] are concerned with efficient algorithms for solving problems of nonlinear deformation and buckling of inhomogeneous shells. Solving nonlinear buckling problems for shells often involves obtaining difficult-to-predict results. They depend on a considerable number of parameters related to the geometry, boundary conditions, load, materials, and structural elements.

The following requirements are imposed on the developed algorithm: universality and capability to efficiently solve a wide class of problems; automatic control of the nonlinear process; automatic following of the load–deflection curve, complex as it may be; self-correction of algorithm parameters, which simplifies the solution process; collection of statistical data in following the load–deflection curve for the analysis and improvement of the algorithm for certain classes of shells; feasibility of complex processes of thermomechanical loading; availability of procedures for processing, visualization, and documentation of the input data and results of solving a nonlinear problem.

The problem of nonlinear deformation, buckling, and postbuckling behavior of inhomogeneous shells is solved by a combined algorithm that employs the parameter continuation method, a modified Newton–Kantorovich method, and a procedure for automatic correction of algorithm parameters [54, 61, 64]. Each step increments (or decrements) the external load parameter P , which is related to the parameters of the mechanical (Q) and temperature (T) fields. The solution of the nonlinear problem is the relationship between the external load parameter P and the displacement field P of the FESM, which is determined at each step of loading ΔP . This relationship is usually represented by a "load – deflection" (" $P - U$ ") curve at characteristic points of the shell.

3.2. Self-Correction of Algorithm Parameters. The efficient automation of the solution algorithm requires implementing the following procedures: selection of the continuation parameter; determination of its rational value; change of the sign of the continuation parameter; determination of the load increment from the displacement increment of a characteristic node; change of the accuracy of the solution of the system of nonlinear equations; change of the patterns and modes of thermomechanical loading at the current step; filing of the input and output data for further documentation, analysis, processing, and visualization. The experience of solving problems for shells under mechanical and thermal loads suggests that the accuracy of the

solution for the latter should be increased by four to five orders of magnitude.

The algorithm is based on the generalized " $P-U$ " curve in the form of a loop with a branching point g and singular points a , b , e , and f (Fig. 5). The linearized matrix of the governing equations degenerates in the neighborhood of these points. The equations are regularized and the singular points are passed by replacing P by U and vice versa at the points $s_1 \div s_5$ defined by the algorithm. To reduce the time it takes the computer to solve the problem, the rational steps for the descent parameter are determined.

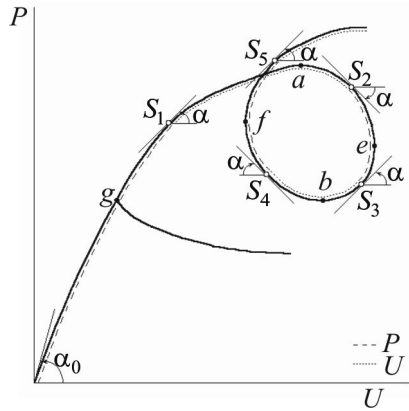


Fig. 5

The algorithm for solving the buckling problem finds the branching points and allows drawing adjacent deformation modes in their neighborhood. To identify a branching point, use is made of a qualitative theory that states that at least one negative eigenvalue of the linearized stiffness matrix represents a new equilibrium configuration of the shell. The adjacent deformation mode is identified by introducing an imperfection defined by the parameter λ into the perfect initial configuration of the shell. If λ is small, its influence is seen near the branching point on the " $P-U$ " curve, which may become critical.

The efficiency of the method is substantially dependent on how it is numerically implemented. The available software packages include poorly developed algorithms for analyzing the geometrically nonlinear deformation, buckling, and postbuckling behavior of shells [65, 66]. Obviously, the reason is that because of their complexity and ambiguity, these problems are difficult to solve with a user-friendly standard computational procedure.

The software package developed is research-oriented and meets the modern requirements to such software regarding input data representation, design models, efficient nonlinear problem-solving algorithm, data processing, analysis, and visualization.

The nodal coordinates of the three-dimensional FESM of arbitrary shape and regular topological structure are determined using a specially developed mesh generator [3, 59, 61, 64].

4. Numerical Analysis of the Convergence and Accuracy of Solutions to Problems of Nonlinear Deformation and Buckling of Inhomogeneous Shells

Of great importance for the development of the FEM is its theoretical justification [26, 27, 37, 43, 56]. This, however, is not sufficient to evaluate the efficiency and applicability of finite-element schemes because asymptotic estimates of accuracy give no indication of their behavior on real, coarse meshes. Not less important is the numerical analysis of the properties of a FE, which is performed by comparing FEM solutions and analytic, numerical, or experimental solutions.

The efficiency, accuracy, and applicability of the method developed were analyzed by solving special linear and nonlinear test problems [6, 32, 50, 61, 64]. Let us consider a number of typical examples.

4.1. Linear Solutions. An analysis of the accuracy of the solutions for homogeneous and inhomogeneous rods, beams, frames, and rings as three-dimensional bodies subject to uniform and nonuniform temperature fields shows rapid convergence on coarse meshes [6, 64]. The results obtained for framed structures and revealed thermoelastic effects can be generalized to thin-walled structures. It is supported by studies on plates and shells.

After that, homogeneous and layered square plates under uniform pressure q are used as examples to determine the errors and possible limits of the elastic constants.

4.1.1. Bending Clamped One-Layer Square Plate. For a clamped one-layer isotropic plate, the central deflection converges rapidly if compared with the analytic solution [57]. Comparing the solution with those obtained with well-known software (LIRA, SCAD, FRONT, ANSYS, NASTRAN, COSMOS) and by other authors, we conclude that the solutions for rectangular plane FEs converge from "above" and the solutions for spatial FEs converge from "below". The same effect is revealed for an orthotropic plate.

It is analyzed the accuracy of the central deflection for two-layer and three-layer simply supported plates [64]. The results are compared with calculations in software SCAD, where it was used multilayer rectangular finite element № 73 [66]. The multilayer FE is absent in software LIRA [65].

4.1.2. Bending Two-Layer Simply Supported Square Plate. We consider the two-layer plate, loaded pressure intensity $q = 0.06 \text{ MPa}$. The central deflection of the plate has been compared to solutions obtained in the software SCAD, by the refined iteratively-analytical theory [21], by the experimental-theoretical method [35] and with the experimental data [35] (Table 1). The input data: a size of the panel in the plan $a = 0.3 \text{ m}$; the first layer (steel) – thickness 0.0003 m , elastic modulus $E = 2.03 \cdot 10^5 \text{ MPa}$, Poisson's ratio

$\nu = 0.3$; the second layer (concrete) – thickness 0.0258 m , $E = 0.0657 \cdot 10^5\text{ MPa}$, $\nu = 0.2$. The design model is a quarter of the panel.

The calculation results of the central deflection of the plate w obtained by different methods have been compared with the experimental data. The solution by MSFE and by SCAD converges rapidly. We conclude that the solutions for MSFE and the iteratively-analytical theory converge to the experimental data from "above" and the solutions for the experimental-theoretical method and software SCAD converge from "below". The significant error is less 10%.

Table 1

Method of analysis	MSFE, 8×8 FEs	SCAD, 8×8 FEs	Iteratively-analytical [21]	Experimental-theoretical [35]	Experimental [35]
$w \cdot 10^2, m$	0.0120	0.0109	0.0115	0.0102	0.0110
$\Delta, \%$	9.10	-0.91	4.5	-7.3	0

Acceptable results are obtained when the ratio of the elastic modules of two layers is equal to 31. This fact should be taken into account when deciding on the areas of possible application techniques.

4.1.3. Bending Three-Layer Simply Supported Square Plate. We consider the three-layer plate [18], loaded pressure intensity $q = 0.1\text{ MPa}$. The input data: a size of the panel in the plan $a = 0.2768\text{ m}$; the 1st and 3rd layers are isotropic with thickness 0.001 m , $E = 6.8 \cdot 10^4\text{ MPa}$, $\nu = 0.3$, $G = 2.615 \cdot 10^4\text{ MPa}$; the 2nd layer is transversely isotropic with thickness 0.015 m , $E = 0.48 \cdot 10^4\text{ MPa}$, $\nu = 0.3$, $G = 0.038 \cdot 10^4\text{ MPa}$. The design model is a quarter of the panel.

Table 2

Method of analysis	MSFE		SCAD		Reissner	Varvak	Engineering theory
	12×12 FEs	16×16 FEs	12×12 FEs	16×16 FEs			
$w \cdot 10^3, m$	0.2354	0.2369	0.3469	0.3475	0.3160	0.3050	0.2160
$\Delta, \%$	-25.5	-25.0	9.78	9.97	0	-3.5	-31.6

The central deflection of the plate w obtained by MSFE has been compared to analytical [18] Reissner's (straight line hypothesis) and Varvak's (tangential stresses and cross-sectional curvature are taken into account) solutions, to the solution produced by the engineering theory (straight normal hypothesis) and to software SCAD (Table 2). Benchmark is the solution obtained by Reissner's theory.

For MSFE and software SCAD refining the mesh from 12×12 FEs weakly corrects the solution (the significant error is respectively about 25 and 10%). The ratio of the elastic modules of material layers (carrier to a placeholder) is 14.2, and the ratio of the shear modules is 68.8. These data should be taken into account when deciding on the areas of possible application of these techniques.

The examples indicate a rough limit of applicability of the method, which corresponds to the well-known statement that the elastic constants of layers should not differ by more than one to two orders of magnitude.

4.2. Solutions in Geometrically Nonlinear Problems of Buckling, and Postbuckling Behavior. Results of research of nonlinear deformation are considered by the example of a number of inhomogeneous isotropic shells. The accuracy of solutions of buckling problems is evaluated by comparing them with nonlinear solutions obtained by other authors and by software LIRA and SCAD [15, 17, 19, 30, 31], which used flat finite elements: triangular № 342 and quadrangular № 344.

"Absolutely rigid insert plates" [65, 68] and "absolutely rigid solids" [44, 66] are used when approximating the shell sections with ribs, channels and cavities, where FEs are joined eccentrically.

4.2.1. A Spherical Panel with Square Planform and Constant Thickness. Panel is hinged along the contour and loaded with uniform normal pressure intensity q [64]. Results are presented in terms of dimensionless parameters: $\bar{q} = a^4 q / (Eh^4)$, $\bar{u}' = u' / h$. Curvature of the panel is defined by parameter $K = 2a^2 / (Rh) = 32$, where: $h = 1$ cm is the thickness, $a = 60h$ is a size of the panel in the plan, $R = 225h$ is the radius of mid-surface, elastic modulus $E = 2.1 \cdot 10^6$ kg/cm², Poisson's ratio $\nu = 0.3$. The FESM is a quarter of the panel with mesh 30×30 FEs. Comparison is made with the solution of [30] by the a "load – deflection" (" $\bar{q} - \bar{u}'$ ") curves at the center of the panel (Fig. 6,a).

The problem has been solved by software LIRA and software SCAD with using its three non-linear algorithms. The upper critical load \bar{q}_{cr}^{up} obtained by software LIRA is in good agreement with the solution [49]: for two variants of the method of successive loadings (SL) discrepancy is less than 3%, the method Newton–Raphson (N–R) gives error -1.8%. This problem with the

software SCAD has been solved by the method Newton–Kantorovich (N–K) and by the method Newton–Raphson (errors -4.9%). Disagreement with the solution by MFES is -3.15%. Equilibrium configurations for the deformed panel in the prebuckling and postbuckling domains for all solutions have a simple form and are in good agreement with each other (Fig. 6,b).

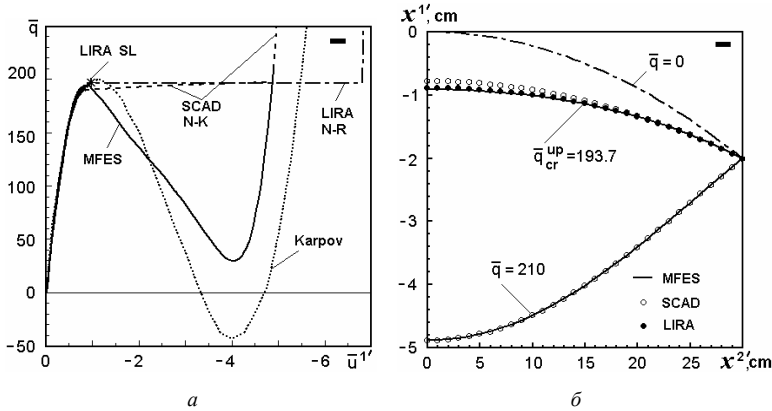


Fig. 6

4.2.2. Shells with Linearly Varying Thickness. The effect on the buckling of the shallow spherical panels of linear variation in the thickness along the meridian is examined, in order to find rational laws of distribution of the material in the volume of construction [61,64]. Shell of revolution clamped at the edge and subjected to uniform normal pressure (Fig. 7,a). The input data: rise $H = 0.05\text{ m}$, radius of mid-surface $R = 10.025\text{ m}$, radius of support boundary $a = 1\text{ m}$, “base” thickness $h^* = 0.01\text{ m}$, $E = 19.6 \cdot 10^4\text{ MPa}$, $\nu = 0.3$.

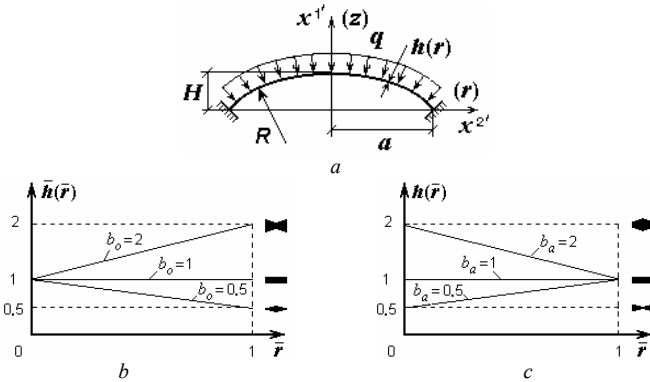


Fig. 7

In general form, we represent the law of linear distribution of thickness along the meridian panel by its thickness in the center $h_{\bar{r}=0}$ and at the edge $h_{\bar{r}=1}$: $h(\bar{r})=h_{\bar{r}=0}+(h_{\bar{r}=1}-h_{\bar{r}=0})\bar{r}$, where $\bar{r}=r/a$. We examine three laws of linear variation in the thickness $h(\bar{r})$ (Fig. 7,b,c; type of variable thickness is indicated by the appropriate icon):

1) $h(\bar{r})=h^*[1+(b_o-1)\bar{r}]$; 2) $h(\bar{r})=h^*[1+(b_a-1)(1-\bar{r})]$; 3) $h(\bar{r})=h^*b_v$, where $b_o=h_{\bar{r}=1}/h_{\bar{r}=0}$, $b_a=h_{\bar{r}=0}/h_{\bar{r}=1}$, $b_v=h_v/h^*$ are parameters characterizing the degree of linear variation in the thickness. The value $b_o=b_a=b_v=1$ corresponds to a panel of constant “base” thickness h^* . The thickness h_v is determined from the volume of a panel V : $h_v=V/(2\pi HR)$.

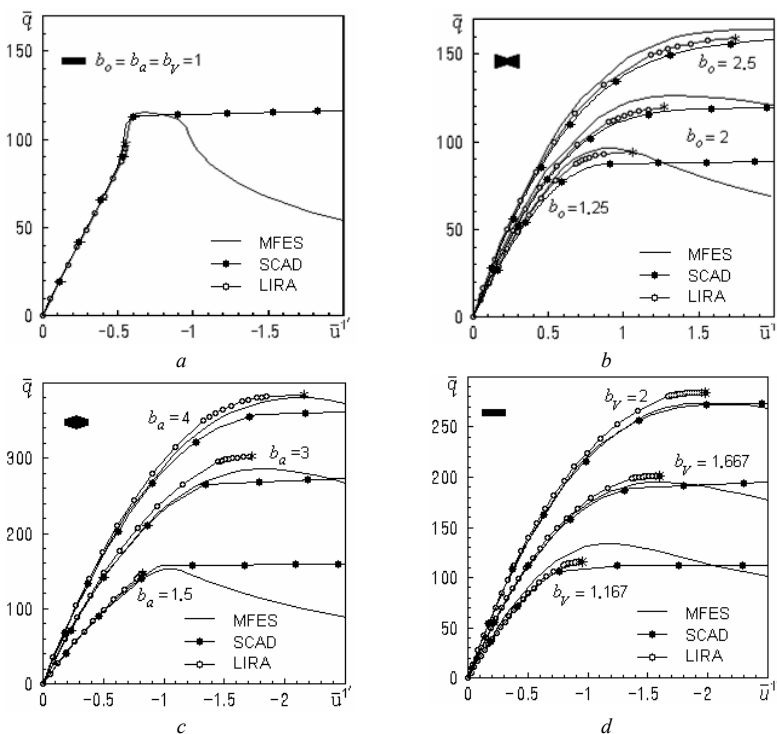


Fig. 8

Consider shells characterizing by equal volumes V with appropriate parameters b_o , b_a , b_V . Solutions obtained by MFES [60,61,64] are compared with those obtained by software LIRA and SCAD. The results are presented in dimensionless form: $\bar{q} = a^4 q / (Eh^{*4})$, $\bar{u}' = u' / h^*$, $\bar{h}(\bar{r}) = h(\bar{r}) / h^*$. Comparing the results reveals complete agreement between the “ $\bar{q}-\bar{u}$ ” curves in the prebuckling domain and in the area of the upper critical point for all solutions (Fig. 8).

4.2.3. Faceted Panels of Stepwise-Varying Thickness. Consider faceted shells formed from the above smooth spherical panels with thickness linearly varying [61,64]. The mid-surface of the spherical shell of revolution is represented by a faceted surface inscribed in it and having 16 flat faces (4×4 for a quarter of the shell, Fig. 9,a). The linearly varying thickness $\bar{h}(\bar{r})$ is replaced by close stepwise-varying thickness \bar{h}_i (Fig. 9,b) according to the range of steel sheets [67] with a permissible in engineering calculations difference of the volumes of these shells (-4.3...+0.2%).

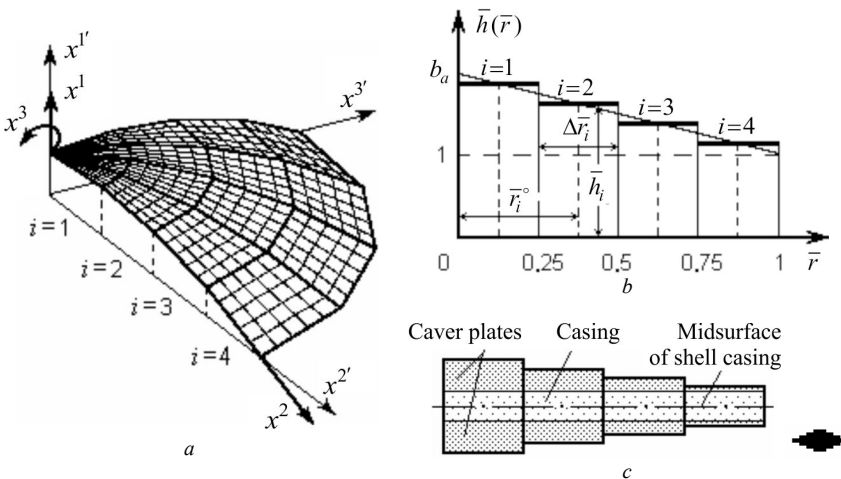


Fig. 9

Nonlinear solutions obtained by MFES are compared with those obtained by software LIRA and SCAD for shells in rational manners [64], which are thicker in the middle. We compare faceted shells with a compound by the mid-surface faces for parameters thickness $b_o = 0.55, 1$ and $b_a = 1, 2, 4$ (Fig. 9,c). We observe well agreement between the “ $\bar{q}-\bar{u}$ ” curves in the prebuckling

domain (Fig. 10). At the branching point for panels with parameters $b_o=0.55$ and $b_o=b_a=1$ difference the load is respectively -0.18 and $+1.98\%$, and for deflections it is $+1.01$ and $+3.5\%$. The upper critical load \bar{q}_{cr}^{up} is in good agreement for panels with parameters $b_a=2$ and 4 (divergence is within -1.91 and 4.17%). At the Fig. 10 to assess the effect faceted, dotted line is shown the solutions obtained by MFES for smooth panel linearly variable thickness.

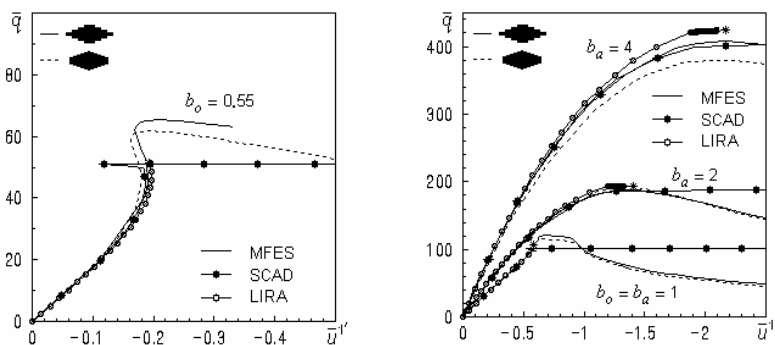


Fig. 10

4.2.4. Ribbed Panels with Square Planform. Investigation of the stability of rib-reinforced shells [61,64] is presented by the example of deep spherical panel square in plan ($K=64$, $a=120h$, $R=450h$), hinged at the edges, and subject to uniform normal pressure (Fig. 11 and 12). Two variants of the shells reinforced ribs from inside (height $h_p=3h$ and width $b_p=2h$) is considered: (i) with two central cross-ribs (with mesh 21×21 FEs) and (ii) with four pairs of equally spaced cross-ribs (with mesh 22×22 FEs).

Solutions obtained by MFES and software LIRA are compared with those obtained by Il'in & Karpov [30]. The “ $\bar{q}-\bar{u}$ ” curves are analyzed: for the first variant (i) at the point “o” (Fig. 11,a) and at the point “b” (Fig. 11,b), and for the second variant (ii) at the center of the shell (Fig. 12,a). For comparison, the dashed-dotted line shows the solution for the smooth panel ($h_p=0$).

The solutions to the first problem (i) obtained by MFES and software LIRA are in good agreement for the “ $\bar{q}-\bar{u}$ ” curves in the prebuckling domain and at the moment of loss of stability (Fig. 11). The difference between the values of \bar{q}_{cr}^{up} for the solution [30] and by MFES is less than 0.5% , the difference for these by MFES and by software LIRA is 1.1% .

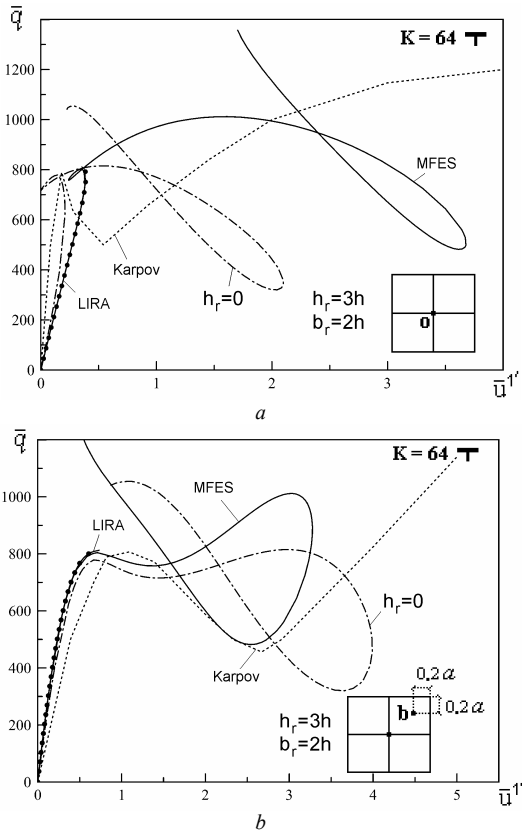


Fig. 11

The solutions to the second problem (ii), for the panel reinforced with either ribs, are in good agreement on all sections of the “ $\bar{q}-\bar{u}$ ” curve. The difference between the values of \bar{q}_{cr}^{up} for the solution [30] and by MFES is -3.8%, the difference for these by MFES and by software LIRA is 7.7%.

Configurations for the deformed panel in the prebuckling (1) and postbuckling (2) domains for all solutions have a simple form and are in good agreement with each other (Fig. 12,b).

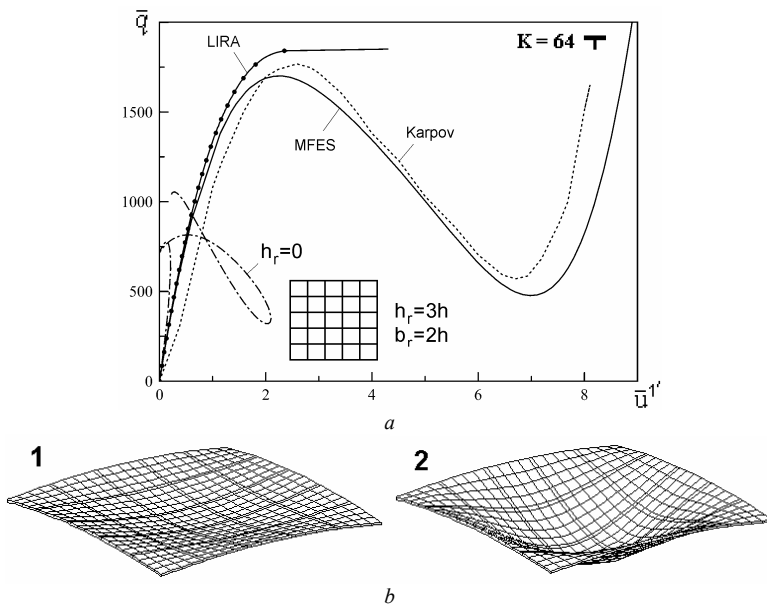


Fig. 12

4.2.5. Panels of Square Planform with Channels and Cavities.

Investigation of the buckling of shells by channels and cavities is presented by the example of a shallow spherical panel square in plan with $K = 32$ [61,64]. It is considered a shell with two variants of non-through weakens: (i) four identical cross channels (width $b_{ch} = 2h$ and depth $h_{ch} = 0.3h$); (ii) four square cavities (width $b_{cv} = 6h$ and depth $h_{cv} = 0.7h$). Three cases of eccentric arrangement of channels and cavities respect to the casing mid-surface are compared (Fig. 13). Each case of the eccentricity is indicated by the appropriate icon. The FESM is a quarter of the panel with mesh 30×30 FEs.

In all cases, solutions obtained by MFES and software LIRA coincide completely in the prebuckling domain and in the domain of the upper critical load (Fig. 13). There is good agreement for the results obtained by MFES, software LIRA and Karpov [30] for panels weakened from inside (Fig. 13, *a, d*). For these panels, the results obtained by software SCAD differ substantially compared with the results of [30] (the error -13.39 and -11.98%), and with the results by MFES (the error -12.03 and -8.61%).

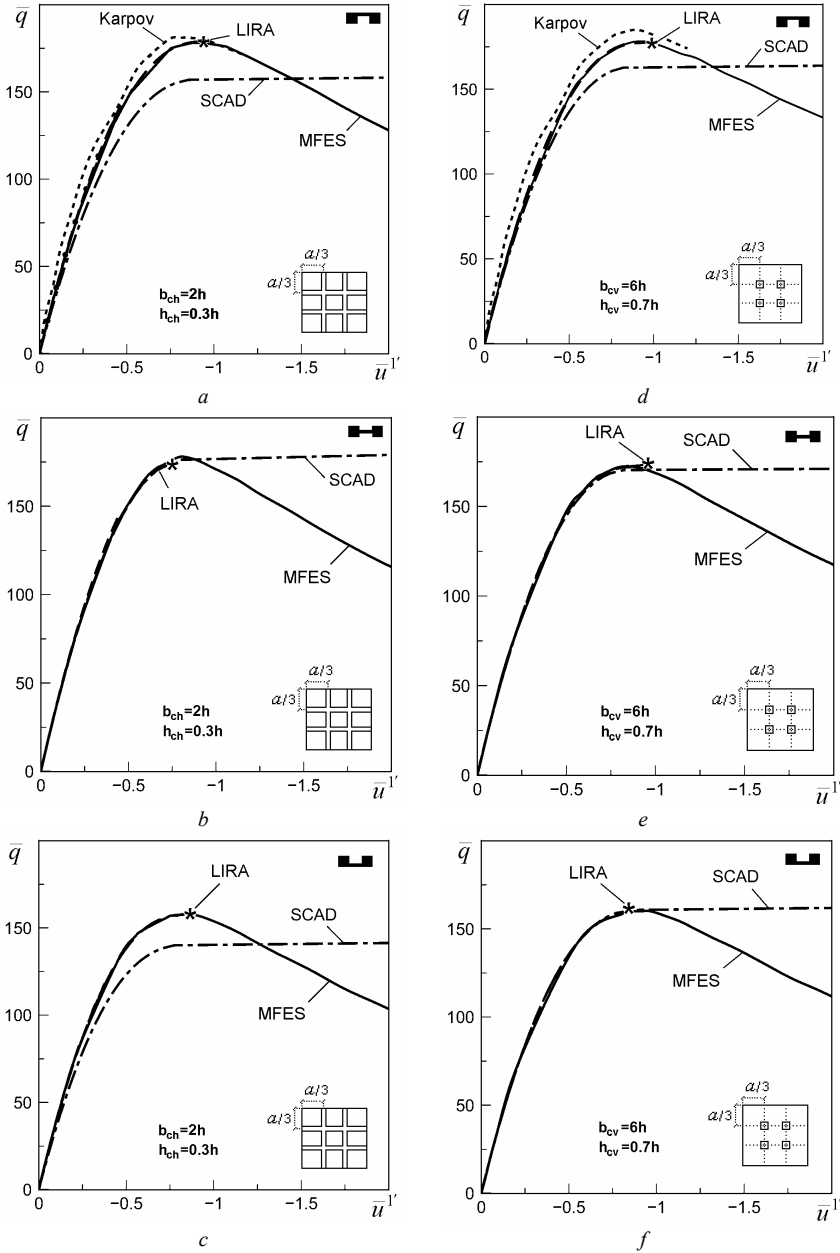


Fig. 13

There is good agreement between the solutions obtained by MFES, software LIRA and SCAD for shells without eccentric arrangement of channels and cavities (Fig. 13, *b, e*). The difference of the results is less than 1%.

4.2.6. Shells under Combined Action of Force and Temperature Fields.

When there are both temperature and force fields, the nonlinear solutions have been analyzed by examples axisymmetric conical panel and square in terms of spherical panel with a hole for a clamped shallow conical round panel in terms [64]. We take into account by MFES and software LIRA that effect of the thermomechanical load occurs in two stages. We have been taken into account by MFES and software LIRA that effect of the thermomechanical load occurs in two stages. At the first stage the shell is gradually heated by the temperature field whose parameter t increases from 0°C to a set value $T^\circ\text{C}$. At the second stage the panel is subjected to uniform normal pressure in addition.

4.2.6.1. Axisymmetric Conical Panel. A clamped shallow conical panel with the radius of support boundary $a = 100h$ and rise $H = 3h$ is considered (Figs. 14). At the first stage of the loading the shell is heated to a set value 20°C [31]. The input data: $h = 0.01\text{ m}$, $E = 19.6 \cdot 10^4\text{ MPa}$, $\nu = 0.3$, linear expansion coefficient $\alpha = 0.125 \cdot 10^{-4}\text{ deg}^{-1}$. Results are presented in terms of dimensionless parameters: $k = H/h$, $\bar{t} = t\alpha(a/h)^2$.

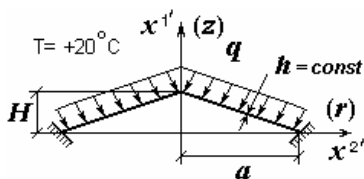


Fig. 14

The design model is a quarter of the panel with mesh 20×40 FEs. Solutions by [31], MFES, and software LIRA are compared.

The considered methods have good agreement the “ $\bar{q} - \bar{u}$ ” curves (Fig. 15,*a*) and forms of deformation (Fig. 15,*b*) at all stages of loading. In the area of the upper critical load there is a discrepancy regarding the solution by MFES: the difference between the values of \bar{q}_{cr}^{up} for software LIRA is 10.8%, and for [31] it is -3.6%.

4.2.6.2. Panel of Square Planform with Hole. A shallow spherical panel ($K=32$, $a=60h$) hinged at the edges and having a central square hole (width $b_h=12h$) is considered. The input data: $h=0.01\text{ m}$, $E=20.59 \cdot 10^4\text{ MPa}$, $\nu=0.3$, $\alpha=0.12 \cdot 10^{-4}\text{ deg}^{-1}$. The design model is a quarter of the panel with mesh 30×30 FEs. The effect of three cases preheating by $T=-20^\circ, 0^\circ, 20^\circ\text{C}$ on the stability of the shell is considered.

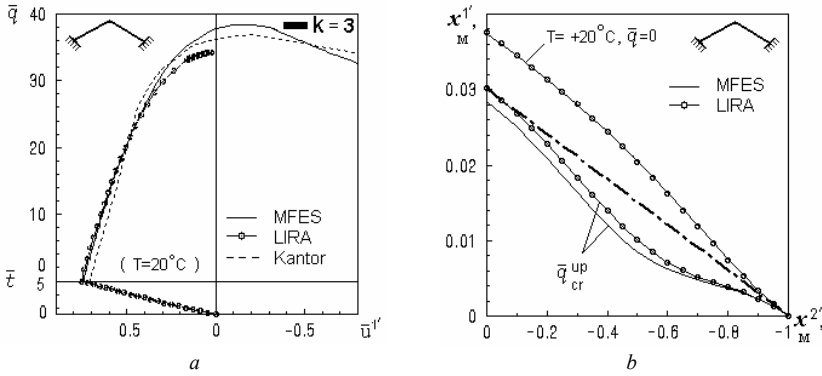


Fig. 15

Fig. 16,a shows a comparison of the “ $\bar{q}-\bar{u}$ ” curves obtained by MSFE, software LIRA and in [31] for shells without hole (■) and with hole (■) when their loading only pressure ($T=0^\circ\text{C}$). For the panel without hole the deflection have been considered at its center. For the panels without hole the deflection have been considered at its center. Comparing the results by MFES and software LIRA reveals agreement between the “ $\bar{q}-\bar{u}$ ” curves in the prebuckling domain and when loss of stability: the difference between the values of \bar{q}_{cr}^{up} is respectively -1.9% and 2.9%. In the area of the upper critical load there is a divergence of the “ $\bar{q}-\bar{u}$ ” curves obtained by MSFE, software LIRA and in [30]: the difference between the values of \bar{q}_{cr}^{up} by MFES and [30] is respectively 3.3 % and -9.9%.

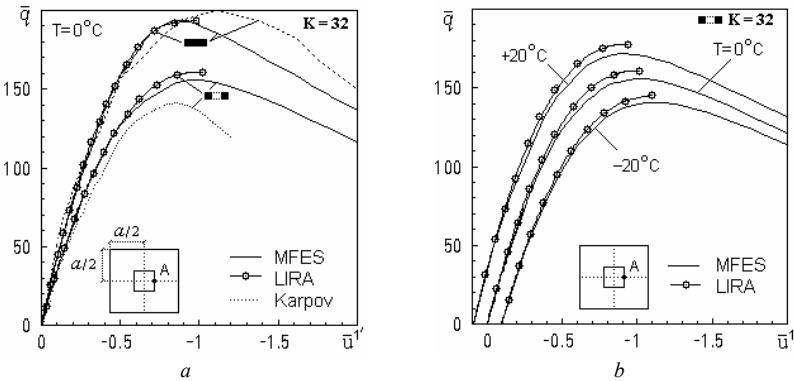


Fig. 16

For all cases of preheating there is agreement between the “ $\bar{q} - \bar{u}$ ” curves in all domains of solutions by MFES and software LIRA (Fig. 16,b). The difference between the values of \bar{q}_{cr}^{up} is within 3.0 – 3.5%, and this for the deflection $\bar{u}_{cr}^{1'up}$ at the point A is within 0.3 – 4.1 %.

Configurations for the deformed panel after pre-cooling to $T = -20^\circ\text{C}$ (Fig. 17,a) and preheating to $T = +20^\circ\text{C}$ (Fig. 17,b) are in good agreement with each other and have little difference from the original form ($T = 0^\circ\text{C}$, $\bar{q} = 0$). Buckling forms are in good agreement too. Buckling of the shell occurs with click of its central part (Fig. 17,c).

Conclusions

We have developed a finite-element method to analyze thin-walled shell structures. The method employs, for all structural elements of an inhomogeneous shell, the geometrically nonlinear equations of the three-dimensional theory of thermoelasticity taking into account all nonlinear terms and components of the strain and stress tensors. Use was also made of the moment finite-element scheme extended to nonlinear thermoelasticity of thin inhomogeneous shells.

We have developed a unified model based on the universal spatial FE that describes the multilayer structure of a material and geometrical features of structural elements of an inhomogeneous shell: casing of varying thickness, ribs, cover plates, cavities, channels, holes, sharp bends of the mid-surface.

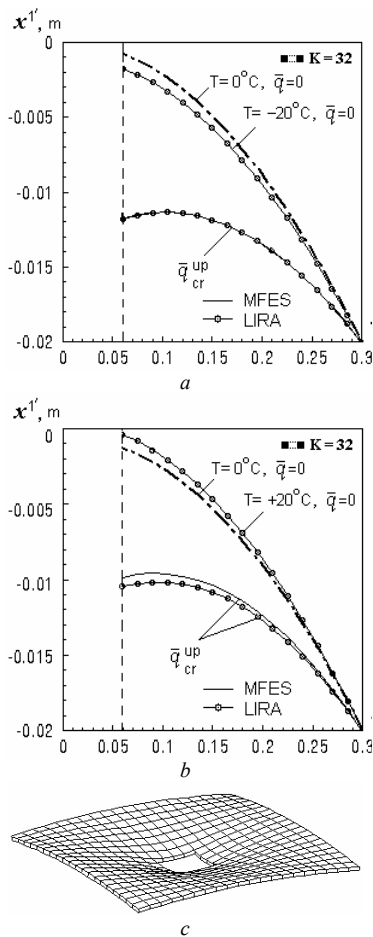


Fig. 17

We have developed an efficient iterative algorithm for solving problems of nonlinear deformation, buckling, and postbuckling behavior of thin inhomogeneous shells under thermomechanical loading.

The reliability of linear and nonlinear solutions for a wide class of inhomogeneous shells has been numerically justified by analyzing their convergence and comparing with those obtained by other authors and by software LIRA and SCAD.

REFERENCES

1. *Alfutov N.A.* Fundamentals of Stability Analysis of Elastic Systems [in Russian], Mashinostroenie, Moscow (1978). 312 p.
2. *Babich D.V.* "Stability of thermosensitive shells nonuniformly heated throughout the thickness," *Dokl. AN Ukrainy*, No. 4, 41–45 (1993).
3. *Bazhenov V.A., Dekhtyaryuk E.S., Solovei N.A., Krivenko O.P.* "Generating finite-element models of complex shells," in: *Proc. Int. Sci. Conf. on Architecture of Shells and Strength Design of Thin-Walled and Engineering Structures of Complex Shape* [in Russian], Izd. RUDN, Moscow (2001), pp. 30–34.
4. *Bazhenov V.A., Krivenko O.P., Solovei M.O.* "Effect of thermomechanical loading conditions on the stability and postbuckling behavior of shells with constant and stepwise-varying thickness" // *Opir Mater. Teor. Sporud*, 77, pp. 30–42 (2005).
5. *Bazhenov V.A., Krivenko O.P., Solovei M.O.* "Stability of conical shells with linearly varying thickness" // *Opir Mater. Teor. Sporud*, 78, pp. 46–51 (2006).
6. *Bazhenov V.A., Krivenko O.P., Solovei M.O.* "Convergence and accuracy of solutions for a spatial finite element in problems of nonuniform heating of rods and beams" // *Opir Mater. Teor. Sporud*, 80, pp. 54–65 (2006).
7. *Bazhenov V.A., Krivenko O.P., Solovei N.A.* "Assessment of the curvature effect on the stability and postbuckling behavior of ribbed panels" // *Strength of Materials*, 39, No. 6, pp. 658–662 (2007).
8. *Bazhenov V.A., Sakharov A.S., Solovei N.A., Krivenko O.P., Ayat N.* "Moment scheme of the finite-element method in problems of the strength and stability of flexible shells subjected to the action of forces and thermal factors" // *Strength of Materials*, 31, No. 5, pp. 499–504 (1999).
9. *Bazhenov V. A., Solovei M. O., and Krivenko O. P.*, "Nonlinear equations of deformation of ribbed thin multilayer shells under thermomechanical loading" // *Opir Mater. Teor. Sporud*, 64, pp. 116–127 (1998).
10. *Bazhenov V.A., Solovei M.O., Krivenko O.P., Ayat N.* "Stability of flexible shells under combined thermomechanical loading," *Opir Mater. Teor. Sporud*, 65, pp. 75–90 (1999).
11. *Bazhenov V.A., Solovei M.O., Krivenko O.P.* "Equations of the moment finite-element scheme in buckling problems for inhomogeneous shells under thermomechanical loading" // *Opir Mater. Teor. Sporud*, 66, pp. 22–25 (1999).
12. *Bazhenov V.A., Solovei N.A., Krivenko O.P.* "Stability of shallow shells of revolution with linearly varying thickness" // *Aviats.-Kosmich. Tekh. Tekhnol.*, No. 2, pp. 18–25 (2004).
13. *Belostotskii A.M.* "Finite-element models of spatial plates, shells, and solids: Creation, program implementation, and research" // *Sb. Nauch. Trudov Hidroproekta*, 100, pp. 24–35 (1985).
14. *Bolotin V.V.* "Nonlinear theory of elasticity and stability in large" // *Rasch. Prochn.*, 3, pp. 310–354 (1958).

15. 15. *Bushnell D., Smith S.* "Stress and buckling of nonuniformly heated cylindrical and conical shells" // AIAA J., 9, No. 12, pp. 2314–2321 (1971).
16. *Vainberg D.V., Gotsulyak E.A., Gulyaev V.I.* "Thermomechanical instability of a deformable medium" // *Sopr. Mater. Teor. Sooruzh.*, 16, pp. 153–156 (1972).
17. *Valishvili N.V.* Methods for Computer Design of Shells of Revolution [in Russian], Mashinostroenie, Moscow (1976). – 278 p.
18. *Varvak P.M., Buzun I.M., Gorodetskii A.S., [et al.].* Finite-Element Method [in Russian], Vysshaya Shkola, Kyiv (1981). – 176 p.
19. *Vol'mir A.S.* Stability of Deformable Systems [in Russian], Nauka, Moscow (1967). – 984 p.
20. *Golovanov A.I., Kornishin M.S.* "Introduction to the finite-element method in statics of thin shells," *Kazan. Fiz.-Tekh. Inst. KF AN SSSR*, Kazan (1990). – 269 p.
21. *Gondlyakh A.V.* "Iterative analytical theory of deformation of multilayer shells" // *Sopr. Mater. Teor. Sooruzh.*, 53, pp. 33–37 (1988).
22. *Grigolyuk É.I. and Kabanov V.V.* Stability of Shells [in Russian], Nauka, Moscow (1978). – 360 p.
23. *Grigolyuk É.I., Shalashilin V.I.* Problems of Nonlinear Deformation: Parameter Continuation Method in Nonlinear Problems of Solid Mechanics, Nauka, Moscow (1988). – 232p.
24. *Grigorenko Ya.M. and Gulyaev V.I.*, "Nonlinear problems of shell theory and their solution methods (review)" // *Int. Appl. Mech.*, 27, No. 10, pp. 929–947 (1991).
25. *Gulyaev V.I., Bazhenov V.A., Gotsulyak E.A.* Stability of Nonlinear Mechanical Systems [in Russian], Vyscha Shkola, Lviv (1982). – 255 p.
26. *Descloix J.* Méthode des Éléments Finis, Suisse, Lausanne (1973). – 95 p.
27. *Johnson M.W. Jr., McLay R.W.* "Convergence of the finite element method in the theory of elasticity" // *ASME, J. Appl. Mech.*, 35, No. 2, pp. 274–278 (1968).
28. *Zienkiewicz O.C.* The Finite-Element Method in Engineering Science, McGraw-Hill, New York (1971).
29. *Zienkiewicz O.C., Irons B.M., Scott F.C., Campbell J.S.* "Three-dimensional stress analysis," in: B.F. de Veubeke (ed.), *High Speed Computing of Elastic Structures*, Universite de Liege (1971).
30. *Il'in V.P., Karpov V.V.* Stability of Ribbed Shells against Large Displacements [in Russian], Stroiizdat, Leningrad (1986). – 168 p.
31. *Kantor B.Ya.* Nonlinear Problems in the Theory of Inhomogeneous Shallow Shells [in Russian], Naukova Dumka (Kyiv) (1974). – 136 p.
32. *Kislookii V.N., Sakharov A.S., Solovei N.A.* "Moment scheme of the finite-element method in geometrically nonlinear problems regarding the strength and stability of shells" // *Strength of Materials*, 9, No. 7, pp. 808–817 (1977).
33. *Koldunov V. A., Kudinov A. N., and Cherepanov O. I.*, "Three-dimensional stability analysis of shells," in: Proc. 6th Int. Sci. Symp. on Modern Problems of Plasticity and Stability in Solid Mechanics (Tver, March 1–3, 2006) [in Russian], TGTU, Tver (2006), pp. 31–39.
34. *Koldunov V.A., Cherepanov O.I.* "Numerical model for design of shells and shell structures using three-dimensional nonlinear theory of elasticity," in: *Complex Systems: Data Processing, Modeling, and Optimization* [in Russian], TvGU, Tver (2002), pp. 48–59.
35. *Kucheryuk V.I., Dorogin A.D., Bochagov V.P.* "Design of multilayer plates by an experimental-theoretical method" // *Sroit. Mekh. Rasch. Sooruzh.*, No. 2, pp. 72–74 (1983).
36. *Liao C.-L., Reddy J.N.* "Analysis of anisotropic stiffened, composite laminates using a continuum-based shell element" // *Comput. Struct.*, 34, No. 6, pp. 805–815 (1989).
37. *Sakharov A.S., Kislookii V.N., Kirichevskii V.V. [et al.].* Finite-Element Method in Solid Mechanics [in Russian], Vyscha Shkola, Kyiv (1982). – 480 p.
38. *Nikolaev A.P., Kiselev A.P.* "Using the three-dimensional theory to design shells," in: Proc. Int. Sci. Conf. on Architecture of Shells and Strength Analysis of Thin-Walled Building and Engineering Structures of Complex Shape [in Russian], Izd. RUDN, Moscow (2001), pp. 29–30.

39. *Nikolaev A.P., Kiselev A.P.* "Design of shells based on three-dimensional finite elements in the form of a triangular prism and octagon," in: Proc. Int. Sci. Conf. on Architecture of Shells and Strength Analysis of Thin-Walled Building and Engineering Structures of Complex Shape [in Russian], Izd. RUDN, Moscow (2001), pp. 319–323.
40. *Nowacki W.* Theory of Elasticity [in Polish], PWN, Warsaw (1970). – 872 p.
41. *Novozhilov V.V.* Theory of Thin Shells [in Russian], Sudpromgiz, Leningrad (1962). – 431 p.
42. *Ogibalov P.M., Gribanov V.F.* Thermal Stability of Plates and Shells [in Russian], Izd. MGU, Moscow (1968). – 520 p.
43. *Oden J.T.* Finite Elements of Nonlinear Continua, McGraw-Hill, New York (1971).
44. *Perel'muter A.V., Slivker V.I.* Design Models of Structures and Possibility to Analyze Them [in Russian], Izd. DMK Press, Moscow (2007). – 600 p.
45. *Piskunov V.G., Verizhenko V.E.* Linear and Nonlinear Problems for Layered Structures [in Russian], Budivel'nyk, Kyiv (1986). – 176 p.
46. *Podstrigach Ya.S., Shvets R.N.* Thermoelasticity of Thin Shells [in Russian], Naukova Dumka, Kyiv (1983). – 343 p.
47. *Rasskazov A.O., Sokolovskaya I.I., Shul'ga N.A.* Theory and Design of Layered Orthotropic Plates and Shells [in Russian], Naukova Dumka, Kyiv (1986). – 191 p.
48. *Rikards R.B.* Finite-Element Method in the Theory of Shells and Plates [in Russian], Zinatne, Riga (1988). – 284 p.
49. *Sakharov A.S.* "A moment finite-element scheme (MFES) that allows for rigid-body displacements" // *Sopr. Mater. Teor. Sooruzh.*, 24, pp. 147–156 (1974).
50. *Sakharov A.S., Solovei N.A.* "Convergence analysis of the finite-element method in problems of plates and shells," // in: *Spatial Structures of Buildings and Installations* [in Russian], Issue 3, Stroizdat, Moscow (1977), pp. 10–15.
51. *Solovei M.O.* "Modeling the thermoelastic properties of multilayer materials in buckling problems for inhomogeneous shells" // *Opir. Mater. Teor. Sporud*, 73, pp. 17–30 (2003).
52. *Solovei M.O.* "A modified three-dimensional finite element for modeling thin inhomogeneous shells" // *Opir. Mater. Teor. Sporud*, 80, pp. 96–113 (2006).
53. *Solovei N.A., Krivenko O.P.* "Comparative analysis of solutions to buckling problems for flexible shells subject to different laws of nonuniform heating" // *Opir. Mater. Teor. Sporud*, 70, pp. 104–109 (2002).
54. *Solovei N.A., Krivenko O.P.* "Influence of heating on the stability of smooth shallow spherical shells with linearly varying thickness" // *Opir. Mater. Teor. Sporud*, 74, pp. 60–73 (2004).
55. *Solovei N.A., Krivenko O.P.* "Influence of heating on the stability of faceted shallow spherical shells" // *Opir. Mater. Teor. Sporud*, 75, pp. 80–86 (2004).
56. *Strang G., Fix G.J.* An Analysis of the Finite-Element Method, Prentice-Hall, Englewood Cliffs (1973).
57. *Timoshenko S.P., Woinowsky-Krieger S.* Theory of Plates and Shells, McGraw-Hill, New York (1959).
58. ANSYS User's Manual for revision 5.6. Vol. I. Procedure; Vol. II. Command; Vol. III. Elements; Vol. IV. Theory.
59. *Solovei N.A.* "Geometrical modelling of shells with complex form by finite element system for strength analysis" // *Prikl. Geometr. Inzhen. Grafika*, 69, pp. 245–251 (2001).
60. *Bazhenov V.A., Solovei N.A.* Nonlinear Deformation and Buckling of Elastic Inhomogeneous Shells under Thermomechanical Loads // *International Applied Mechanics*, 2009 [in Russian]. – Vol. 45. – № 9. – Pp. 3–40.
61. *Bazhenov V.A., Solovei N.A.* Nonlinear Deformation and Buckling of Elastic Inhomogeneous Shells under Thermomechanical Loads // *International Applied Mechanics*, 2009. – Vol. 45. – № 9. – Pp. 923–953.
62. *Bazhenov V.A., Krivenko O.P., Solovei N.A.* Nonlinear Deformation and Buckling of Elastic Shells with Inhomogeneous Structure [in Ukraine] – ZAT «Vipol», (Kyiv), 2010. – 316 p.

63. *Bazhenov V.A., Solovei N.A.* Nonlinear Deformation and Buckling of Elastic Inhomogeneous Shells under Thermomechanical Loads // **Mechanics successes in 6 volumes**. Vol. 6 (book 2). – Litera LTD (Kyiv), 2012. – Pp. 609-645.
64. *Bazhenov V.A., Krivenko O.P., Solovei N.A.* Nonlinear Deformation and Buckling of Elastic Shells with Inhomogeneous Structure: Models, Methods, Algorithms, Poorly Studied and New Problems [in Russian]. – Book House "LIBRIKOM" (Moscow), 2013. – 336 p.
65. LIRA 9.4 User Guide. Basics. Textbook. / *Strelets- Streletsky E.B., Bogovis V.E., Genzersky Y.V., Geraymovich Y.D., [et al.]*. – Izd. "Fact" (Kyiv), 2008. – 164 p.
66. SCAD Office. Software SCAD. / *Karpilovsky V.S., Kriksunov E.Z., Perel'muter A.V., Perel'muter M.A.* – Izd. "SCAD SOFT" (Moscow), 2009 [in Russian]. – 656 p.
67. GOST 82-70 (ST SEV 2884-81). Steel mill universal broadband. Assortment. – Instead of GOST 82-57; introduced. 1.1.72. – Publishing House of Standards, " (Moscow), 1983. – 6 p.
68. *Gorodetski A.S., Evzerov I.D.* Computer models of structures. – Izd. "Fact" (Kyiv), 2007. – 394 p.

Стаття надійшла до редакції 23.12.2013 р.

Баженов В.А., Соловей М.О., Кривенко О.П.

МОДЕЛЮВАННЯ НЕЛІНІЙНОГО ДЕФОРМУВАННЯ ТА ВТРАТИ СТІЙКОСТІ ПРУЖНИХ НЕОДНОРІДНИХ ОБОЛОНОК

Викладено основи метода розв'язування статичних задач геометрично нелінійного деформування, стійкості та закритичної поведінки тонких пружних неоднорідних оболонок, що мають складну форму серединної поверхні, геометричні особливості за товщиною, багатопшарову структуру матеріалу та знаходяться в умовах складного термосилового навантаження. Підхід базується на геометрично нелінійних співвідношеннях тривимірної теорії термопружності та використанні моментної схеми скінчених елементів. Дано чисельне обґрунтування метода. Виконано порівняння розв'язків з розв'язками інших авторів і в програмних комплексах ЛІРА, SCAD

Ключові слова: геометрично нелінійне деформування, стійкість, тонка пружна неоднорідна оболонка, термосилове навантаження.

Баженов В.А., Соловей Н.А., Кривенко О.П.

МОДЕЛИРОВАНИЕ НЕЛИНЕЙНОГО ДЕФОРМИРОВАНИЯ И ПОТЕРИ УСТОЙЧИВОСТИ УПРУГИХ НЕОДНОРОДНЫХ ОБОЛОЧЕК

Изложены основы метода решения статических задач геометрически нелинейного деформирования, устойчивости и закритического поведения тонких упругих неоднородных оболочек, имеющих сложную форму срединной поверхности, геометрические особенности по толщине, многослойную структуру материала и находятся в условиях сложного термосилового нагружения. Подход основан на геометрически нелинейных соотношениях трехмерной теории термоупругости и использовании моментной схемы конечных элементов. Дано численное обоснование метода. Выполнено сравнение решений с решениями других авторов и в программных комплексах ЛИРА, SCAD.

Ключевые слова: геометрически нелинейное деформирование, устойчивость, тонкая упругая неоднородная оболочка, термосиловая нагрузка.